Spatial Variations in Growth Rate within *Klebsiella pneumoniae* Colonies and Biofilm

Eric J. Wentland,[†] Philip S. Stewart,[*,†] Ching-Tsan Huang, and Gordon A. McFeters[‡]

Center for Biofilm Engineering and Departments of Chemical Engineering and Microbiology, Montana State University, Bozeman, Montana 59717

The use of acridine orange to visualize and quantify spatial variations in growth rate within *Klebsiella pneumoniae* colonies and biofilm was investigated. Bacterial colonies supported on polycarbonate filter membranes were grown on R2A agar plates. Some colonies were sampled for cell enumeration, while others were cryoembedded, sectioned, and stained with the fluorescent nucleic acid stain acridine orange. Spatial patterns of fluorescent color and intensity with depth in the colony were quantified using confocal microscopy and image analysis of stained cross sections. Colonies sampled in the midexponential phase were thin (20 μm), had high average specific growth rates (>1 h^{-1}), and had all the cells stained bright orange. Colonies sampled after more than 24 h of growth were thick (>200 μm) and were growing slowly (μ < 0.15 h^{-1}). These older colonies were characterized by distinct bands of orange at the colony edges and a dark green center. Stained biofilm cross sections displayed a similar orange band at the biofilm−bulk fluid interface and a green interior. Colony-average specific growth rates, determined by calculating the local slope of the cell accumulation versus time data, were correlated with colony-average fluorescence intensities. There was no correlation betweeen average specific growth rate and orange or green intensity individually, but growth rate did correlate with the orange:green intensity ratio (r^2 = 0.57). The resulting regression was used to predict specific growth rate profiles within colonies. These profiles indicated that bacteria were growing rapidly near the air and agar interfaces and more slowly in the center of the colonies when thicker than about 30 μm. The dimension of the orange bands ranged from 10 to 30 μm, which may indicate the thickness of growing regions. The inherent variability associated with this technique suggests that it is best applied in single species systems and that the results should be regarded as qualitative in nature.

Introduction

Our research group has been investigating explanations for the much reduced susceptiblity of biofilm microorganisms, when compared to freely suspended cells, to killing by antimicrobial agents. A better understanding of the fundamental mechanisms involved in biofilm resistance could help guide the development of more effective strategies for biofouling control in diverse systems including cooling water, drinking water distribution, secondary oil recovery, paper manufacturing, and medical implants.

Evidence is mounting in support of a transport-based explanation for the failure of biocides to effectively disinfect biofilms (Chen et al., 1993; de Beer et al., 1994; Stewart and Raquepas, 1995; Xu et al., 1996). According to this hypothesis, the biocide fails to fully penetrate the biofilm because it is neutralized by reaction with constituents of the biofilm faster than it diffuses in. This mechanism appears to be plausible for reactive biocides, such as chlorine. A second explanation for biofilm recalcitrance to chemical challenge turns on physiological differences between biofilm and suspended microorganisms (Brown and Gilbert, 1993). It is quite reasonable to postulate that microorganisms deep within a biofilm, where the chemical microenvironment might be quite different from that in the bulk fluid, will be physiologically disinct and thereby less susceptible to disinfection. In particular, slow growing or starving microorganisms in the interior of the biofilm are candidates for reduced susceptibility (Brown et al., 1988; Tresse et al., 1995). It is this scenario that motivates this article.

Approaches that have been used to characterize microbial growth rates in immobilized cell and biofilm systems include nucleic acid staining (Monbouquette and Ollis, 1988; Monbouquette et al., 1990), radioisotope labeling (Stewart and Robertson, 1988; Stewart et al., 1991), immunofluorescent recognition of pulse-labeled DNA (Kuhn et al., 1991, 1993), and oligonucleotide probing of ribosomal RNA content (Delong et al., 1989; Kerkhof and Ward, 1993; Poulsen et al., 1993).

Nucleic acid staining has attractive features. RNA to DNA ratios have been found to correlate with specific growth rate in many different bacteria, and fluorescent stains are commonly used to perform these measurements on planktonic organisms (Rosset et al., 1966; Delong et al., 1989; Moyer et al., 1990; Berdalet and Dortch, 1991; Kemp et al., 1993; Kerkhof and Ward, 1993; Poulsen et al., 1993). In addition, no expensive or hazardous labeling compound need be introduced into the bioreactor: the stain is applied to a small sample ex-situ. In preliminary screening experiments, we have identified acridine orange as an attractive candidate stain for use

[†] Department of Chemical Engineering.
[‡] Department of Microbiology.
* Corresponding author.

S8756-7938(96)00024-0 CCC: $12.00

with biofilm or immobilized bacteria (McFeters et al., 1991). Advantages of this stain are that it is membrane permeant and that RNA and DNA both stain but fluoresce at different wavelengths (650 and 526 nm, respectively). The two nucleic acid pools can thus be measured simultaneously in the same microscopic field.

The purpose of the work reported in this article was to evaluate acridine orange staining as a means for visualization and quantification of spatial patterns of growth rate within microbial aggregates.

Materials and Methods

Microorganism and Media. Pure cultures of *Klebsiella pneumoniae* were used throughout. Fresh batch cultures were prepared as innoculum for each colony growth experiment. A defined glucose minimal medium was used for batch cultures (Chen et al., 1993). Cultures were grown at room temperature overnight to obtain a final cell concentration of approximately 1×10^5 cfu/mL prior to inoculating membranes. Plates of R2A agar (Difco) or R2A agar with glucose omitted were used in colony growth experiments.

Colony Growth Procedure. Colonies of *K. pneumoniae* were grown on top of filter membranes resting on agar plates. Black polycarbonate filter membranes (Poretics Corp.) with a pore size of 0.2 μm and a diameter of 25 mm were used for all colony growth experiments. Membranes were wrapped in aluminum foil and sterilized by autoclaving at 121 °C for 15 min. Sterile membranes were then asceptically placed on the agar surface with the shiny side of the membrane facing up. In a typical experiment, 20−25 membranes (one membrane per plate) were used. Each filter membrane was inoculated with one 5 μL drop from an overnight batch culture. For aerobic growth experiments, agar plates with inoculated filter membranes were kept at 35 °C in a conventional incubator. For anaerobic growth experiments, agar plates were placed in a nitrogen-filled anaerobe tent (Coy, Model 12356, Ann Arbor, MI) overnight before inoculation. Temperature in the tent ranged from 34 to 40 °C. In both aerobic and anaerobic experiments, membranes were periodically sampled to determine viable cell counts as well as for cryoembedding.

Cell Enumeration. Bacteria were enumerated by aseptically removing a filter membrane from the surface of the agar and placing it in a test tube containing 9 mL of phosphate buffer. The forceps used to remove the filter membrane from the surface of the agar were treated sequentially in 10 mg/L chlorine bleach, 1% sodium thiosulfate, and filter-sterilized distilled water prior to lifting the membrane. The test tube was then vortexed for 5 min in order to remove cells from the surface of the filter. The resulting suspension was serially diluted in sterile phosphate buffer. Colony-forming units were determined using a drop plate method on R2A agar.

Determination of Average Specific Growth Rate. Growth curves representing the number of colony-forming units on individual filter membranes as a function of time were used to determine colony-average growth rates. A least-squares line was regressed to at least three sequential data points at various stages of the growth curve to ascertain the growth rate at a particular point in time. Typically this procedure was applied to cell count data obtained from a duplicate membrane sampled at the same time that a colony was collected for embedding and staining along with two (or more) additional cell count data points from neighboring sample times. Often, more than three points were used in determining the regression, and whenever applicable, more data points (cfu samples) prior to the sample time of the stained colony cross section were used than after the time of the stained sample. The slope of the regressed line was taken as the growth rate for that sample.

Embedding and Sectioning. A croyembedding technique was used to preserve the structure of bacterial colonies for sectioning (Yu et al., 1994). Colonies were embedded by aseptically removing a filter membrane from the surface of the agar and placing it directly on dry ice (CO_2). The bacterial colony was covered with a small drop of colored embedding agent (Cryochrome, Shandon) that served as a marker. After the colored embedding agent was frozen, the membrane was covered with a clear embedding agent (Tissue-Tek OCT compound, Miles Inc.). When the embedding agent was frozen, the polycarbonate filter membrane was removed by carefully peeling it away from the frozen embedding agent. The colony was then turned over, and the bottom of the colony was embedded. The embedded colony was stored at −70 °C until sectioning.

Embedded colonies were sectioned using a cryostat (Reichert-Jung Cryocut 1800, Leica). The embedded colony was transferred to the cryostat and allowed to reach thermal equilibrium at −19 °C. The colony was then placed on the chuck and sectioned. Cuts perpendicular to the plane of the colony were made through the specimen using a disposable miroctome blade (No. 815, Reichert-Jung, Leica) until the colored marker was observed. Subsequent 5 μm thick cross sections were placed on polylysine-coated microscope slides (Superfrost Plus, Fisher Scientific) and examined under phase contrast microscopy to confirm that the bacterial colony was contained within the cross section.

Fixation and Staining. Colony cross sections were fixed for 10 min at 4 °C in a fixative consisting of 10% formaldehyde, 5% glacial acetic acid, and 85% ethanol. Slides were then rinsed with two changes of 85% ethanol and allowed to air dry. Fixed sections were stored under refrigeration. A stock solution of 200 mg/L acridine orange (Sigma) in phosphate buffer (pH 7.2) was formulated and incubated at 35 °C overnight. The stock solution was then filtered through a 0.2 μm syringe filter (Acrodisc, Gelman Sciences) to remove any undissolved particulates. From the stock solution, a fresh solution of 4 mg/L acridine orange in phosphate buffer was prepared for colony staining. Colonies were stained by locating the cross section on the glass slide and placing 2 μL drops in succession along the length of the cross section. Sections were stained for 5 min, then excess staining solution was blotted from the slide.

Microscopy. Stained sections were analyzed using a MRC Bio-Rad confocal scanning laser microscope equipped with a krypton/argon laser. The colony was scanned 5 times using the Kalman setting with 10% transmission. Images were captured and stored. Stored images were then analyzed using the Mark image analysis software (Harkin and Shope, 1993).

Photomicrographs were taken with an Olympus BH-2 microscope with epifluorescent illumination. Olympus B filter cubic unit with excitation filter BP490, dichroic mirror DM500, and barrier filter AFC + O515 was used.

Image Analysis. Digitized confocal images were imported into the Mark software and analyzed for variations in color and intensity across the colony. Colony images were oriented by their placement on the microscope stage so that the agar side of the colony was parallel to the ordinate with the abscissa corresponding to the width of the cross section. The intensities of each column of pixels were averaged to get an average intensity profile across the width of the colony.

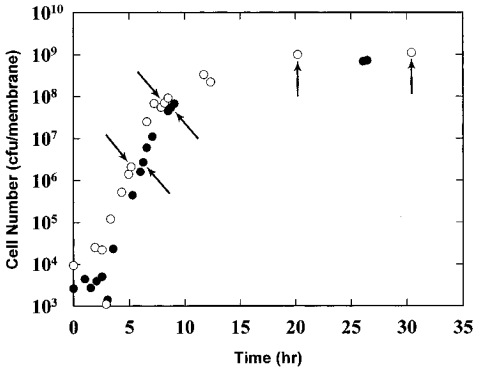

Figure 1. *K. pneumoniae* colony growth aerobically on R2A agar at 35 °C. Results from duplicate experiments dated 11-16-94 (●) and 11-22-94 (○) are shown. Arrows indicate times when a duplicate membrane was sampled and cryoembedded.

Intensity profile data represented the average pixel intensity of each pixel column at each wavelength (526 nm (green) and 650 nm (orange)) after staining the colony. The first step in analyzing image data was to determine which data values represented colony fluorescence and which values represented background fluorescence. The image profile from the orange fluorescence was graphed (average intensity vs pixel column), and the points at the bottom of the curves where the slopes increased and decreased at the greatest rates were considered the boundaries of the colony. If the curve from the orange values did not give a clear indication of the colony boundaries, green intensity values were used for this purpose. The mean pixel intensity across the entire cross section was determined for both the green and orange intensities. This was done by averaging the intensity values within the colony boundaries.

The average orange intensity value was divided by the corresponding average green intensity value. Each intensity ratio value corresponded to a specific sample time which had an estimated growth rate associated with it. The ratio value was then plotted versus its respective growth rate.

Biofilm Growth Procedure. In one experiment, pure culture biofilm of *K. pneumoniae* was grown in a continuous flow annular reactor as described elsewhere (Murga et al., 1995). Briefly, biofilm was developed on stainless steel slides using a defined minimal medium with 40 mg/L glucose as the sole carbon and energy source. The dilution rate in the reactor was 3.2 h^{-1}. Frozen sections of biofilm were obtained from biofilm covered slides harvested after 7 days of reactor operation by a procedure detailed previously (Murga et al., 1995). Subsequent staining and microscopic analysis protocols were identical to those described above for membrane-supported colonies.

Results and Discussion

Colony Growth. *K. pneumoniae* accumulated in colonies growing aerobically on R2A agar as shown in Figure 1. Bacteria grew exponentially for approximately 8 h, then entered a phase of reduced and steadily declining growth rate. Estimates of the average colony growth rates at the sampling times indicated in Figure 1 of 5.2, 8.2, 20.2, and 30.4 h were 1.7, 0.56, 0.16, and 0.086 h^{-1}, respectively (Table 1).

The biphasic colony growth curves measured suggest an exponential phase of accumulation followed by a linear, transport-limited phase. The transport limitation could be for oxygen (supplied from the air side), a carbon source (supplied from the agar side), or both. Transition from exponential phase to transport-limited phase typically occurred after 7−10 h when the colony was approximately 10−30 μm thick. Once the colony has entered the transport-limited phase, spatial gradients in the physiology and growth rate of bacteria within the colony are to be expected.

Table 1. Summary of Average Specific Growth Rates and Growing Region Dimensions

expt date	O_2	glucose	time (h)	growth rate (h^{-1})	colony total (μm)	agar side (μm)	air side (μm)
11-16-94	yes	yes	6.25	1.87	42		22
			8.75	0.93			
			26.50	0.14			
11-22-94	yes	yes	5.17	1.7			
			8.17	0.56	97	20	19
			20.20	0.16			
			30.42	0.086	240	13	13
12-15-94	yes	no	7.00	1.22			
			8.83	0.61			
			13.13	0.10			
			23.87	0.10			
12-30-94	yes	no	6.08	1.16			
			8.22	0.41			
			10.93	0.25			
			27.58	0.11	125	16	16
11-30-94	no	yes	8.20	0.54			
			10.28	0.20			
			24.12	0.053			
			27.08	0.053			
12-07-94	no	yes	6.75	0.59			
			8.62	0.34	28	12	19
			29.25	0.028			
			49.77	0.28	162	28	11
1-10-95	no	yes	8.23	0.60			
			10.17	0.15			
			24.00	0.044			
			26.00	0.044			
			32.00	0.044			
			33.90	0.044			

Acridine Orange Staining. When embedded colonies were sectioned, stained with acridine orange, and examined using epifluorescence microscopy, temporal and spatial patterns in staining color and intensity were observed (Figure 2). A colony sampled and stained midway through the exponential growth phase (5.2 h) was thin and all the cells appeared bright orange (Figure 2A). The colony-average specific growth rate at this sampling time was 1.7 h^{-1}. As a colony began to make the transition from exponential to transport-limited growth (after 8.75 h), gradients in fluorescent color could be observed (Figure 2B). The colony appeared more orange close to the air and agar interfaces and was yellow or greenish yellow in the middle. Yellow-green color was most evident in the thickest parts of the colony. The average colony growth rate for the sample shown in Figure 2B was 0.93 h^{-1}. A colony sampled after 26.5 h was thick with distinct bands of orange at the colony edges and a dark green center (Figure 2C). The colony-average growth rate of the specimen pictured in Figure 2C was 0.14 h^{-1}. At higher magnification, orange cells can be seen lining the convolutions and channels within the colony. In an old (49.8 h) anaerobically grown colony, an orange band is apparent along the agar interface with a fainter yellow-orange band at the gas (N_2) interface (Figure 2D). The average growth rate for the specimen in Figure 2D was 0.028 h^{-1}.

A biofilm embedded, sectioned, and stained with acridine orange yielded images similar to those obtained from colonies (Figure 2E). The biofilm was green in the interior with an orange band running along the biofilm−bulk fluid interface. In places where the biofilm was locally thin, the orange band extended to the substratum.

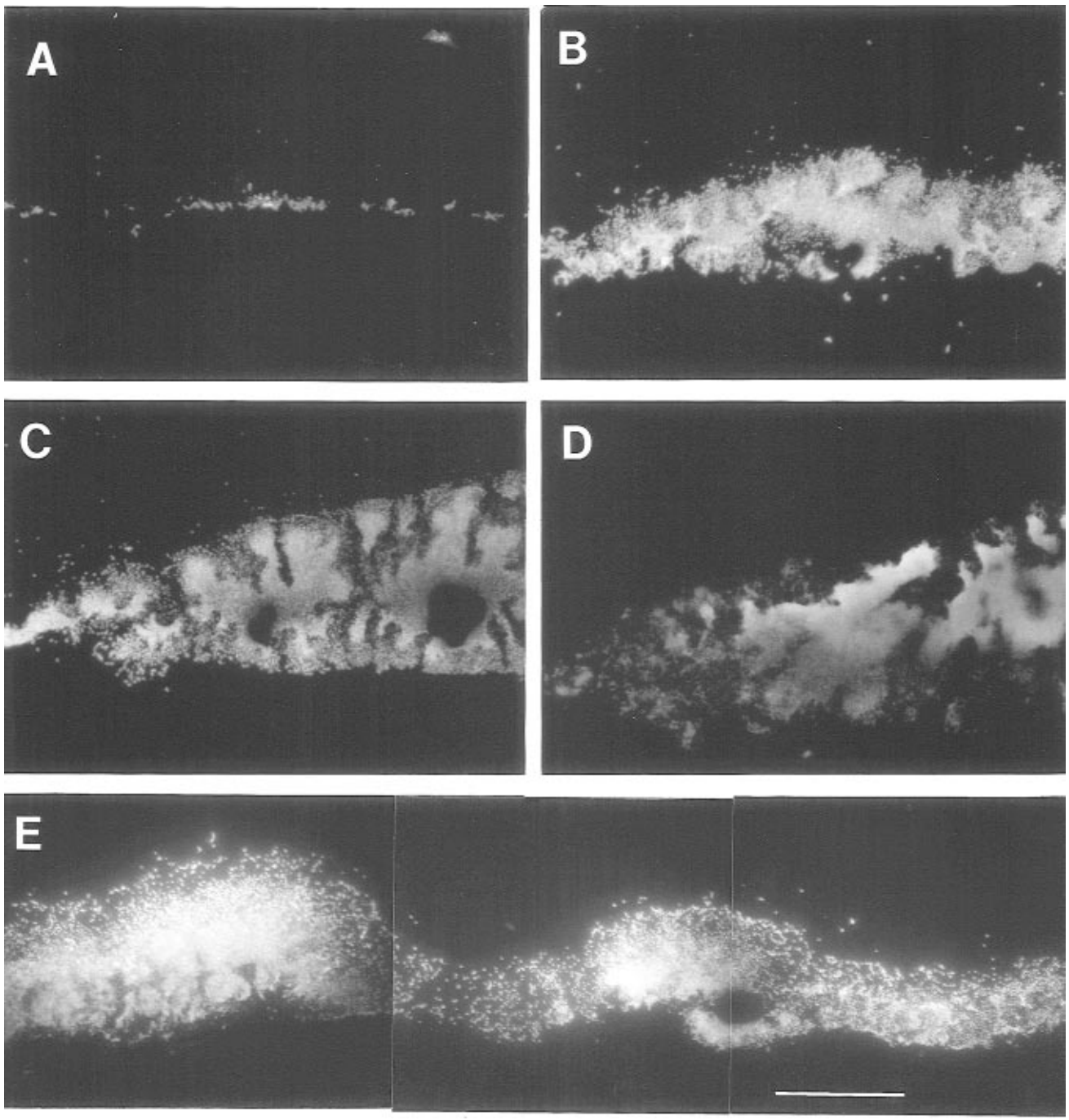

Figure 2. Photomicrographs of portions of acridine orange stained cross sections of *K. pneumoniae* colonies and biofilm. The growth conditions and colony ages were (A) aerobic, 5.17 h; (B) aerobic, 8.75 h; (C) aerobic, 26.5 h; (D) anaerobic, 49.77 h old. The cross sections are oriented such that the air side of the colony was at the top and the membrane (agar) side of the colony at the bottom of each picture. Panel E shows a section of biofilm grown in continuous culture. In panel E, the bulk fluid was at the top and the substratum at the bottom. The scale bar is 100 μm.

The reactor average specific growth rate of the biofilm microorganisms in this experiment, as calculated from an overall cell balance, was 0.16 ± 0.05 h^{-1}.

The photographs in Figure 2 immediately suggest that orange color corresponds to regions of rapid growth and green to regions of slow growth. There is a plausible explanation for such a relationship in the well-known metachromatic staining of nucleic acids by acridine orange. The dye fluoresces orange when bound to single-stranded nucleic acids and green when bound to double-stranded nucleic acids. Because RNA is predominantly in a single-stranded form whereas DNA is predominantly double stranded, the staining color gives an indication of the relative proportions of RNA and DNA in the cell. Fast growing cells, in which the RNA to DNA ratio is relatively large, would tend to appear orange, whereas slow growing cells, with a smaller RNA to DNA ratio, appear yellow or green. Our results do not address the intermediate mechanisms relating staining color and growth rate, but they are consistent with the known interaction of acridine orange with nucleic acids and with the well-established correlation between RNA:DNA ratio and specific growth rate.

The fact that orange bands were observed at both the agar and air sides of the colony suggests dual substrate limitations in the colony. The limitation is presumably for oxygen with increasing depth from the air side, while the limitation is likely for a fermentable carbon source in the R2A medium, such as glucose or soluble starch, in the opposite direction. In the middle of older colonies,

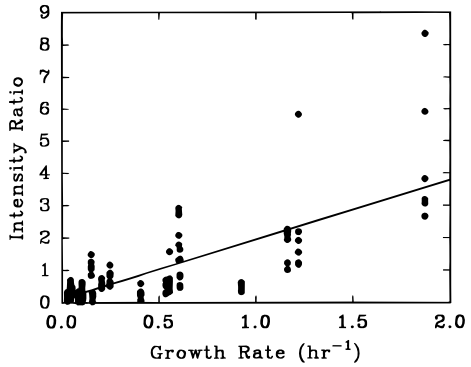

Figure 3. Comparison of average orange:green intensity ratio and colony-average specific growth rate. The regressed line shown is given by $y = 1.84x + 0.107$ ($r^2 = 0.57$).

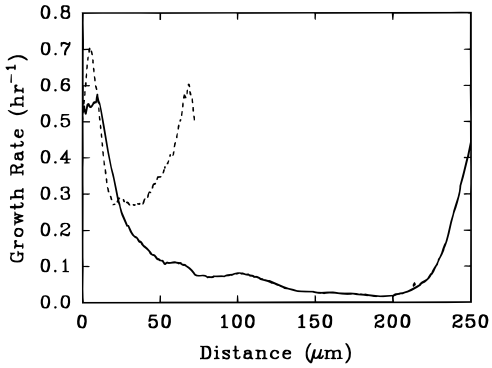

Figure 4. Estimated growth rate profiles in aerobically grown colonies. The colony ages and average specific growth rates were 30.42 h old, 0.086 h^{-1} (—) and 8.17 h old, 0.56 h^{-1} (- - -). The membrane interface (agar side) was at approximately zero on the x axis.

where specimens stained green with acridine orange, cells were probably experiencing deprivation of both oxygen and of fermentable substrates. Aerobic growth is possible at the air interface because there are nonfermentable carbon sources in the medium. Orange bands were also observed at the gas interface in colonies grown in an anaerobe tent (Table 1, Figure 2D). The most likely explanation for this is that the anaerobe tent functioned imperfectly, allowing enough oxygen in to permit some aerobic growth.

Staining Intensity/Growth Rate Correlation. The relationship between staining color intensity and measured specific growth rate was investigated. To do this, the color gradations apparent in Figure 2 were quantified by collecting digitized intensity profiles of colony cross sections. The orange to green intensity ratio profile was then obtained by dividing the average orange intensity of each pixel column by its corresponding average green intensity. When such intensity ratio profiles were obtained, we consistently found higher values close to the air−colony and agar−colony interfaces and smaller intensity ratio values in the colony interior. Intensity ratios varied between zero and nine with a mean of approximately 0.8.

Colony-average fluorescent intensities, obtained by averaging data in 4−6 profiles from a single colony, were compared to colony-average specific growth rates determined from cell count data. There was poor correlation between average growth rate and orange ($r^2 = 0.014$) or green intensity ($r^2 = 0.19$) alone, but growth rate did correlate positively with the orange:green intensity ratio ($r^2 = 0.57$; Figure 3).

Using the linear regression of data in Figure 3 and profiles for the orange:green intensity ratio, spatial variations in the growth rate across a colony cross section were estimated (Figure 4). These profiles indicated that bacteria were growing rapidly near the air and agar interfaces and more slowly in the center of colonies. Referring for example to Figure 4, a 70 μm thick colony yielded maximum local growth rates near the agar and air interfaces of approximately 0.7 and 0.6 h^{-1}, respectively. The minimum growth rate of about 0.3 h^{-1} occurred in the middle of the colony. A 250 μm thick colony displayed slightly lower peak growth rates of approximately 0.5 h^{-1} and a much lower minimum growth rate (<0.05 h^{-1}) in the center of the colony.

The correlation presented in Figure 3 is consistent with the differential staining of RNA and DNA by acridine orange and the known dependence of bacterial RNA:DNA ratio on specific growth rate. Similarly, estimated growth rate profiles (e.g., Figure 4) are at least qualitatively consistent with the pattern of growth expected under conditions of diffusive transport limitation of nutrients or oxygen.

We noted considerable variability in the color obtained when staining biofilm sections with acridine orange. Staining color depended on the concentration of acridine orange, the bacterial species, the fixative, and the recent nutritional status of the bacteria. The staining concentration used, 4 mg/L, was selected after preliminary studies with concentrations ranging from 2 to 200 mg/L. Low concentrations of acridine orange yielded greener specimens, while high concentrations shifted the staining color to orange. The concentration of 4 mg/L was selected because it produced the best contrast between green and orange in mature colony cross sections. The optimal staining concentration is likely to be species specific. In staining two species biofilms containing *Pseudomonas aeruginosa* in addition to *K. pneumoniae*, complex staining patterns were obtained that were not easily interpreted. We also attempted nutrient shift experiments in which colonies on membranes were transferred from an R2A plate to a moist filter pad (downshift). After several hours of starvation, the colony was transferred back to a fresh R2A plate (upshift). The staining results from these experiments (data not shown) were highly variable and could not be easily interpreted. These observations along with the inherent scatter apparent in the correlation shown in Figure 3 suggest that this technique is only applicable to single-species systems grown in relatively stable environmental conditions.

Growing Region Dimensions. The dimensions of growing regions within colonies were estimated by calculating the width of the peak half-heights of the growth rate profiles. They ranged from 11 to 28 μm. For aerobic experiments, the growing region on the agar side of the colonies appeared to have approximately the same thickness as the growing region on the air side of the colonies (Table 1).

The dimension of the air side growing region approximates the estimated depth of oxygen penetration into the colony. Wimpenny and Coombs (1983) used an oxygen microelectrode to measure oxygen penetration depths of 25−30 μm in agar-supported bacterial colonies. The penetration depth can also be estimated from reaction−diffusion theory. For zero-order oxygen utilization kinetics, the penetration depth, a, is given by

$$a = \left(\frac{2S_o Y_{xs} D_e}{\mu X}\right)^{1/2}$$

From this equation, the aerobic layer thickness was

calculated to be 25 μm using the following parameter estimates: oxygen concentration at colony−agar interface, S_o, 7 g/m^3 (saturation concentration at Bozeman, MT, elevation); yield of biomass on oxygen, Y_{xs}, 0.7 g/g; effective diffusion coefficient of oxygen in colony, D_e, 2.6 $\times$ 10^{-5} cm^2/s (80% of aqueous diffusion coefficient at 35 °C); specific growth rate, μ, 1.8 h^{-1} (Table 1); cell density, X, 8 $\times$ 10^4 g/m^3. Thus, the experimentally measured growing region dimensions on the air side of colonies were consistent with the expected transport limitation of oxygen.

The growing region thickness in the biofilm experiment, as estimated from the dimension of the orange band in photomicrographs (Figure 2E), was approximately 30−50 μm.

Conclusions

A technique to visualize and quantify the spatial pattern of nucleic acid staining within bacterial colonies and biofilms was developed. Acridine orange stained colony and biofilm cross sections gave spatial variations in color and intensity apparently associated with variations in growth rate. Orange staining, corresponding to rapid growth, occurred preferentially near the air and agar interfaces of colonies and near the biofilm−bulk fluid interface of biofilm. Green staining, corresponding to slow growth, predominated in the colony and biofilm interior. A quantitative relationship between orange to green fluorescent intensity ratio and growth rate was developed. The correlation between fluorescent intensity ratio and growth rate was significant but not strong enough to make accurate predictions of the absolute values of growth rates based on staining. The inherent variability associated with this technique suggests that it is best applied in single-species systems and that the results should be regarded as qualitative in nature.

Acknowledgment

This research was supported through cooperative agreement EEC-8907039 between the National Science Foundation and Montana State University. We thank Gayle Callis for preparation of frozen sections.

Literature Cited

Berdalet, E.; Dortch, Q. New double-staining technique for RNA and DNA measurement in marine phytoplankton. *Mar. Ecol.: Prog. Ser.* **1991**, *73*, 295−305.

Brown, M. R. W.; Gilbert, P. Sensitivity of biofilms to antimicrobial agents. *J. Appl. Bacteriol. Symp. Suppl.* **1993**, *74*, 87S-97S.

Brown, M. R. W.; Allison, D. G.; Gilbert, P. Resistance of bacterial biofilms to antibiotics: a growth-rate related effect? *J. Antimicrob. Chemother.* **1988**, *22*, 777−783.

Camper, A. K. In *Biofouling and Biocorrosion in Industrial Water Systems*; Geesey, G. G., Lewandowski, Z., Flemming, H.-C., Eds.; Lewis Publishers: Boca Raton, FL, 1993; pp 91−105.

Chen, C. I.; Griebe, T.; Characklis, W. G. Biocide action of monochloramine on biofilm systems of *Pseudomonas aeruginosa*. *Biofouling* **1993**, *7*, 1−17.

de Beer, D.; Srinivasan, R.; Stewart, P. S. Direct measurement of chlorine penetration into biofilms during disinfection. *Appl. Environ. Microbiol.* **1994**, *60*, 4339−4344.

Delong, E. F.; Wickham, G. S.; Pace, N. R. Phylogenetic stains: ribosomal RNA-based probes for identification of single cells. *Science* **1989**, *243*, 1360−1363.

Harkin, G.; Shope, P. The Mark image analysis system. Technical report, Center for Biofilm Engineering, Montana State University, Bozeman, MT, 1993.

Kemp, P. F.; Lee, S.; LaRoche, J. Estimating the growth rate of slowly growing marine bacteria from RNA content. *Appl. Environ. Microbiol.* **1993**, *59*, 2594−2601.

Kerkhof, L.; Ward, B. B. Comparison of nucleic acid hybridization and fluorometry for measurement of the relationship between RNA/DNA ratio and growth rate in a marine bacterium. *Appl. Environ. Microbiol.* **1993**, *59*, 1303−1309.

Kuhn, R.; Peretti, S.; Ollis, D. Microfluorimetric analysis of spatial and temporal patterns of immobilized cell growth. *Biotechnol. Bioeng.* **1991**, *38*, 340−352.

Kuhn, R.; Peretti, S.; Ollis, D. Acid inhibition of immobilized cells: quantitative comparison of model and experiment. *Appl. Biochem. Biotechnol.* **1993**, *39/40*, 401−413.

McFeters, G. A.; Singh, A.; Byun, S.; Callis, P. R.; Williams, S. Acridine orange staining reaction as an index of physiological activity in *Escherichia coli*. *J. Microbiol. Methods* **1991**, *13*, 87−97.

Monbouquette, H. G.; Ollis, D. F. Scanning microfluorimetry of Ca-alginate immobilized *Zymomonas mobilis*. *Bio/Technology* **1988**, *6*, 1076−1079.

Monbouquette, H. G.; Sayles, G. D.; Ollis, D. F. Immobilized cell biocatalyst activation and pseudo-steady state behavior: model and experiment. *Biotechnol. Bioeng.* **1990**, *35*, 609−629.

Moyer, C. L.; Mordy, C. W.; Carlson, D. J.; Morita, R. Y. Ethidium homodimer used for the sensitive measurement of DNA and RNA of a psychrophilic marine bacterium grown at different growth rates during starvation-survival. *J. Microbiol. Methods* **1990**, *12*, 75−81.

Murga, R.; Stewart, P. S.; Daly, D. Quantitative analysis of biofilm thickness variability. *Biotechnol. Bioeng.* **1995**, *45*, 503−510.

Perry, R. H.; Chilton, C. H. *Chemical Engineer's Handbook*, 5th ed.; McGraw-Hill: New York, 1973.

Poulsen, L. K.; Ballard, G.; Stahl, D. A. Use of rRNA fluorescence in situ hybridization for measuring the activity of single cells in young and established biofilms. *Appl. Environ. Microbiol.* **1993**, *59*, 1354−1360.

Rosset, R.; Julien, J.; Monier, R. Ribonucleic acid composition of bacteria as a function of growth rate. *J. Mol. Biol.* **1966**, *18*, 308−320.

Stewart, P. S.; Raquepas, J. B. Implications of reaction-diffusion theory for the disinfection of microbial biofilms by reactive antimicrobial agents. *Chem. Eng. Sci.* **1995**, *50*, 3099−3104.

Stewart, P. S.; Robertson, C. R. Product inhibition of immobilized *Escherichia coli* arising from mass transfer limitation. *Appl. Environ. Microbiol.* **1988**, *54*, 2464−2471.

Stewart, P. S.; Karel, S. F.; Robertson, C. R. Characterization of immobilized cell growth rates using autoradiography. *Biotechnol. Bioeng.* **1991**, *37*, 824−833.

Tresse, O.; Jouenne, T.; Junter, G.-A. The role of oxygen limitation in the resistance of agar-entrapped, sessile-like *Escherichia coli* to aminoglycoside and betalactam antibiotics. *J. Antimicrob. Chemother.* **1995**, *36*, 521−526.

Xu, X.; Stewart, P. S., Chen, X. Transport limitation of chlorine disinfection of *Pseudomonas aeruginosa* entrapped in alginate beads. *Biotechnol. Bioeng.* **1996**, *49*, 93−100.

Yu, F. P.; Callis, G. M.; Stewart, P. S.; Griebe, T.; McFeters, G. A. Cryosectioning of biofilms for microscopic examination. *Biofouling* **1994**, *8*, 85−91.

Wimpenny, J. W. T.; Coombs, J. P. Penetration of oxygen into bacterial colonies. *J. Gen. Microbiol.* **1983**, *129*, 1239−1242.

Accepted February 28, 1996.[⊗]

BP9600243

[⊗] Abstract published in *Advance ACS Abstracts,* May 1, 1996.